Food & Function

ROYAL SOCIETY OF CHEMISTRY

PAPER

View Article Online
View Journal | View Issue



Cite this: *Food Funct.*, 2023, **14**, 4607



# *Moringa oleifera* leaf polysaccharides exert anti-lung cancer effects upon targeting TLR4 to reverse the tumor-associated macrophage phenotype and promote T-cell infiltration†

Shukai Wang,‡ Qian Hu,‡ Zihao Chang, Yuqi Liu, Ye Gao, Xiaowei Luo, Lipeng Zhou, Yinxin Chen, Yitong Cui, Zhaohui Wang, Baojin Wang, Ya Huang, Yue Liu,* Runping Liu * and Lanzhen Zhang*

Received 29th November 2022,
Accepted 22nd April 2023

DOI: 10.1039/d2fo03685a

rsc.li/food-function

Tumor-associated macrophages (TAMs) participate in tumorigenesis, growth, invasion as well as metastasis by facilitating an immunosuppressive tumor microenvironment. Reversing the pro-tumoral M2 phenotype of TAMs has become a hot spot in advancing cancer immunotherapy. In the current study, the content of *Moringa oleifera* leaf polysaccharides (MOLP) was determined and characterized, along with the anti-cancer mechanism of MOLP studied in a Lewis lung cancer (LLC) tumor-bearing mouse model and bone marrow-derived macrophages. The monosaccharide composition and gel permeation chromatography analyses show that MOLP are mainly composed of galactose, glucose, and arabinose, with approximately 17.35 kDa average molecular weight ($M_w$). *In vivo* studies demonstrate that MOLP convert TAMs from the immunosuppressive M2 phenotype to the antitumor M1 phenotype, thus inducing CXCL9 and CXCL10 expression and increasing T-cell infiltration in the tumor. Furthermore, macrophage depletion and T cell suppression demonstrated that the tumor suppressive effect of MOLP was reliant on reprogramming macrophage polarization and T cell infiltration. *In vitro* studies revealed that MOLP could induce the phenotypic switch from M2 macrophages to M1 by targeting TLR4. The current study highlights that MOLP are promising anticancer plant-derived polysaccharides with potential in modulating the immune microenvironment and have a bright application prospect in the immunotherapy of lung cancer.

## 1. Introduction

Lung cancer, which can be categorized into non-small cell lung cancer (NSCLC) and small cell lung cancer (SCLC), is one of the most widespread malignancies with the highest incidence and mortality rates worldwide.[1] NSCLC, primarily squamous cell carcinoma and adenocarcinoma, is responsible for 80–85% of all lung carcinoma cases, and most NSCLC patients are already in the advanced disease stage when diagnosed.[2] Despite the drastic research efforts to develop effective treatments for lung cancer, such as chemotherapy, targeted therapies, and combination regimens, the incidence and mortality of the disease have not decreased significantly.[3]

There is growing evidence that the tumor microenvironment (TME) plays a critical role in tumor progression, including local drug resistance, immune escape, and cancer metastasis,[4] and hence, immunotherapy aiming to reverse or reeducate the TME has achieved certain success in treating various types of cancers.[5] As a complicated tumor ecosystem, the TME is predominantly composed of tumor cells, stromal cells, immune cells, and the extracellular matrix.[6] As the progression of cancer is regulated by the interaction between tumor cells and the tumor site environment, efforts to develop anti-cancer therapies are no longer just traditionally focused on inhibiting tumor cell proliferation. Tumor-associated macrophages (TAMs) are the major infiltrating cells in the tumor immune microenvironment.[7] Activated macrophages have two polarized states: classically activated M1-like macrophages and alternatively activated M2-like macrophage subtypes. The M1-like macrophages participate in antigen presentation and phagocytic clearance of tumor cells. Instead, M2-like macrophages exhibit a vigorously immunosuppressive phenotype to support tumor cell proliferation.[8] Studies have shown that in the TME, TAMs are usually educated by tumor

*School of Chinese Materia Medica, Beijing University of Chinese Medicine, Beijing 102488, PR China. E-mail: liuyuebei_002@163.com, liurunping@bucm.edu.cn, zhanglanzhen01@126.com*

†Electronic supplementary information (ESI) available. See DOI: https://doi.org/10.1039/d2fo03685a

‡These authors contributed equally to this work.

cells as co-conspirators and are phenotypically considered mainly as M2 macrophages.[9] Therefore, it is generally accepted that the discovery of effective drugs to selectively promote M1 polarization of TAMs is a promising therapeutic strategy for malignancies.[10]

Plant polysaccharides are widely found in nature and have multiple biological activities, including anti-tumor, immunomodulatory, hypoglycemic, antioxidant, anti-radiation, *etc*.[11] Compared with other drugs, natural polysaccharides act as biological response modifiers (BRM) that produce broad immune enhancement chiefly through activation of the host's immune system, both innate and acquired immunity.[12] They show little cytotoxicity in humans and have great potential for combination therapy.[13] Various available polysaccharides have shown their anti-tumor properties. For instance, *Dendrobium officinale* polysaccharides significantly inhibit tumor growth in multiple tumor-bearing mice by targeting the TLR2 receptor of TAMs to facilitate TAM polarization toward the M1 phenotype.[14] Apple polysaccharides prevent colitis-associated carcinogenesis by modulating macrophage polarization.[15]

*Moringa oleifera* leaf refers to the leaves of the *Moringa oleifera* tree, a tropical deciduous perennial tree native to India.[16] Polysaccharides of *Moringa oleifera* leaf (MOLP) have been identified as potential immunoregulators as they enhance the production of M1 phenotype-related genes interleukin-6 (IL-6) and tumor necrosis factor-α (TNF-α) in RAW 264.7 cells,[17] suggesting that MOLP may have the ability to polarize M2 phenotype TAMs into the anti-tumor M1 phenotype. However, little research has been conducted to identify the possible anti-tumor effects of MOLP.

Our current study utilizes a Lewis lung cancer (LLC) xenograft mouse model to investigate the anti-tumor effects of MOLP and explore the underlying immunoregulatory mechanisms and further demonstrated that MOLP inhibited tumor growth by binding the TLR4 receptor to polarize TAMs toward the M1 phenotype, thereby promoting the infiltration of cytotoxic lymphocytes and reeducating the immunosuppressive TME.

## 2. Materials and methods

### 2.1 Chemicals and reagents

Standards (fucose, rhamnose, glucose hydrochloride, amino galactose hydrochloride, arabinose, galactose, glucose, xylose, mannose, ribose, galacturonic acid and glucuronic acid) were obtained from Huaster Bio-Technology Co, Ltd (Wuhan, China). All organic solvents used were at least of analytical grade. In addition, all reagents, chemicals, and solvents were purchased from commercial sources unless otherwise stated.

### 2.2 Sample preparation and characterization

*Moringa oleifera* leaves were purchased from Anhui Jiu li Xiang Pharmaceutical Co., Ltd (Anhui, China), and identified by Professor Chunsheng Liu, School of Chinese Materia Medica, Beijing University of Chinese Medicine. Leaves were first washed with deionized water, followed by drying at 60 °C. Dried samples were further crushed using a pulverizer, and passed through a 0.3 mm metal sieve for storage at 4 °C. The crude polysaccharides were obtained through hot water extraction as well as ethanol precipitation based on previous studies[18] with some modifications. Briefly, powder of the dried *Moringa oleifera* leaves (500 g) was extracted twice with water (12.5 L) at 90 °C. The crude extract was centrifuged, filtered, and concentrated. The extracts were precipitated by anhydrous ethanol and the crude polysaccharides were collected by centrifugation. Subsequently, the precipitate was redissolved to dialyzed for 24 h at ambient temperature using MWCO 3500 Da dialysis bags. Post dialysis, the retentate was deproteinated twice using the Savage method.[19] The fractions were collected, precipitated, and finally lyophilized to obtain MOLP.

The total protein, carbohydrate, and uronic acid contents in the MOLP were determined by the Coomassie Brilliant Blue G-250 dye-binding method,[20] the phenol–sulfuric acid method[21] and the carbazole–sulfuric acid method,[19] respectively. High performance liquid gel permeation chromatography (HPGPC),[22] PMP derivatized polysaccharide hydrolysate method,[23] scanning electron microscopy,[24] and infrared spectroscopy analysis[25] of the molecular weight, monosaccharide composition, microstructure and main functional groups were performed, respectively.

### 2.3 Cell culture and viability

LLC and RAW 264.7 cell lines were cultured in Dulbecco's modified Eagle's medium (DMEM) supplemented with 10% heat-inactivated fetal bovine serum (FBS) plus 1% penicillin–streptomycin, maintained at 37 °C in a humid environment containing 5% $CO_2$.

Cell proliferation was measured by a Cell Counting Kit-8 (CCK-8) assay. Briefly, cells were seeded in quadruplicate on 96-well plates and incubated overnight under the standard conditions to allow cell attachment. Then, the cells were treated with MOLP in concentrations of 0 to 1000 μg $mL^{-1}$ and incubated for 24 hours. After adding 10 μL of CCK-8 (Lablead, Beijing, China) to each well and incubating at 37 °C for 2 h, the cell viability was calculated based on the OD values at 450 nm.

### 2.4 Acquisition and polarization of BMDMs *in vitro*

Referring to previous studies,[26] to harvest bone marrow-derived macrophages (BMDMs), femurs and tibias were first isolated from 8-week-old C57BL/6 mice, followed by flushing bone marrow with a 1 mL syringe, separating cells from the bone into RPMI 1640 medium and filtering through a 70 μm cell strainer to remove bone, hair and other tissues. Next, the cells were centrifuged at 500*g* for 10 min. Finally, cells were inoculated into 6-well tissue culture plates containing RPMI 1640 medium with 10% FBS and 10% L929 supernatants, and the medium was changed every 3 days.

Cell polarization conditions were as follows: M1: 100 ng $ml^{-1}$ LPS (L2880, Sigma-Aldrich), M2: 10 ng $mL^{-1}$ recombinant mouse IL-4 and 10 ng $mL^{-1}$ recombinant mouse IL-13

 

(PeproTech, Rocky Hill, NJ, USA). For tumor education, the cell culture medium was collected from the LLC cancer cell line and incubated in a serum-free medium for 24 h and added to BMDMs for 24 h on day 7.

### 2.5 Conditioned medium preparation

Different polarized macrophages were cultured in a serum-free medium for 24 h. The conditioned media of M2 BMDM (BCM) and three different concentrations of MOLP of treated or untreated M2 macrophages were collected, centrifuged at 1000*g* for 5 min and stored at −20 °C until use.

### 2.6 Animal experiments

All the animal experiments were approved by the Institutional Animal Care and Use Committee at Beijing University of Traditional Chinese Medicine, Beijing, China (approval code no. BUCM-4-2022111502-4040), and conducted in compliance with the local animal welfare laws, guidelines and policies. Six-week-old female C57BL/6 mice were purchased from Beijing SPF (Beijing) Biotechnology Co., Ltd (Beijing, China). Animals were acclimatized to laboratory conditions (22 °C ± 1 °C, humidity (40 ± 5%), 12–12 h light–dark cycle, and free access to food and water) 1 week before the experiment and fasted 24 h before operation. To establish a tumor model, LLC cells ($1 \times 10^6$ per mouse) were inoculated subcutaneously in the left axilla of C57BL/6 mice, respectively. When the tumor size reached approximately 5 mm in length, the mice were randomly divided into three groups (6 mice per group) and treated with distilled water or MOLP (0.5 or 1 g $kg^{-1}$ per day, oral gavage) for 12 days, respectively. Mice were executed by cervical dislocation after 12 days and the tumor tissues were collected. The tumor size and weight of the mice were monitored once every 3 days, while the tumor volume was determined based on the following equation: length × $width^2$ × 0.5.

Clodronate liposomes (CL) were used primarily for macrophage depletion; in short, CL (Sunnipo, Shanghai, China) were taken out of a refrigerator and restored to room temperature (20 °C). The CL were mixed 8 times upside down and 200 μL of PL was injected intraperitoneally into each mouse. Macrophages were depleted twice a week for 2 weeks. Regarding immunosuppression, tacrolimus (1 mg $kg^{-1}$, TargetMol) was given intraperitoneally on alternate days.

### 2.7 Quantitative real-time PCR

Total RNA was isolated by using a FastPure Cell/Tissue Total RNA Isolation kit (Vazyme), following the manufacturer's protocol. cDNA was synthesized from 1 μg of total RNA with the HiScript III RT SuperMix for qPCR (+gDNA wiper) (Vazyme) and quantitative real-time polymerase chain reaction (qRT-PCR) was performed using a Bio-Rad CFX96 real-time system (Bio-Rad, USA) by using the Taq Pro Universal SYBR qPCR Master Mix (Vazyme), following the manufacturer's instructions. The mRNA expression of each sample was calculated by normalization with HPRT-1 as an endogenous control. All reactions were performed in triplicate and the relative gene expression was calculated on a comparative threshold cycle (Ct) method.[27] The primer sequences are presented in Table S1.†

### 2.8 Tumor digestion and flow cytometry

Tumor tissues were excised as well as digested with 1 mg $mL^{-1}$ collagenase I (Biorigin) and 0.2 mg $mL^{-1}$ DNase I (Biorigin) for 30 min at 37 °C. After termination of digestion with DMEM containing 5% FBS, the tumor cells were passed through a 70 μm filter and the resulting filtrate was centrifuged at 850*g* for 5 min, and the tumor cells were washed with PBS containing 2 mM EDTA twice.

Tumor single cell suspensions or BMDMs were stained with PE/Cyanine7-CD11b (Biolegend, cat#101215), PE-F4/80 (Biolegend, cat#123109), AF488-CD86 (Biolegend, cat#105017) and APC-CD206 (Biolegend, cat#141707) antibodies for 40 min at 4 °C in the dark, and then washed with PBS twice and resuspended in PBS. Finally, the single-cell suspensions after staining were analyzed using a BD FACS Canto II.

### 2.9 Histology and immunohistochemistry

All tissues were fixed in 4% paraformaldehyde for 24 h at room temperature, imbedded in paraffin, cut into slices of 5 μm thickness, de-paraffinized, and rehydrated for hematoxylin and eosin (H&E) staining and immunohistochemical processing.

Concerning immunohistochemistry, the de-paraffinized sections were heated in an antigen repair solution (Servicebio, Beijing, China) (pH 9.0) for 15 min and then cooled to room temperature. Endogenous peroxidase was incubated in 3% hydrogen peroxide for 25 min, protected from light, followed by rinsing with PBS. Slides were blocked in 3% BSA for 30 min at room temperature before incubation overnight at 4 °C with primary antibodies (anti-iNOS, anti-cleaved caspase-3, anti-CD206, anti-CD68, anti-CD31, anti-CD4 and anti-CD8, Servicebio, China). After incubation with HRP-conjugated secondary antibodies for 50 min at room temperature, the sections were stained with diaminobenzidine (DAB) and the nuclei were counterstained with hematoxylin.

### 2.10 Statistical analysis

Results were displayed as mean ± SEM and were subject to analysis by one-way analysis of variance (ANOVA), followed by Tukey's multiple comparison *post hoc* test; $p$ values <0.05 were regarded as statistically significant.

## 3. Results

### 3.1 Chemical composition and characterization of MOLP

After a series of steps including water extraction, alcoholic precipitation, deproteinization as well as dialysis, a crude polysaccharide of 3.1 g was obtained from the powder of *Moringa oleifera* leaves, yielding 6.2%. Chemical composition analysis showed that MOLP contained 72.13% ± 1.06% total sugar, 1.22% ± 0.21% proteins, and 2.69% ± 0.27% glyoxylates (Table S2†). HPLC analysis determined that polysaccharides were composed of diverse monosaccharides, with galactose,

glucose, and arabinose accounting for the highest content of 44.60%, 24.19%, and 16.93%, respectively (Fig. 1A and B). Infrared spectroscopy is a powerful tool for characterizing the feature groups of organic compounds. As shown in the IR spectrum, polysaccharides have two distinctive absorption bands: O–H and C–H stretching vibrations have absorption bands at 3400 $cm^{-1}$ and 2923 $cm^{-1}$, respectively. The absorption peaks in the range of around 1100 to 1000 $cm^{-1}$ were attributed to C–O–C and C–O–H vibrations, suggesting the presence of pyranose. The featured absorption bands at 898 $cm^{-1}$ and 846 $cm^{-1}$ revealed that both α and β conformations of the sugar unit may be present in MOLP (Fig. 1C). The results of gel permeation chromatography showed that MOLP have a relatively homogeneous molecular weight with an average molecular weight of 17.345 kDa (Fig. 1D). Scanning electron microscopy images (Fig. 1E and F) offer intuitive evidence of the varied morphological profiles of the polysaccharides. They show that the surface of MOLP is relatively rough, with many fine protruding particles and irregular pores, and exhibits a honeycomb-like porous structure. This interconnection of polysaccharide molecules to form a pore-like morphology is presumed to be correlated with the interaction between the multi-branched polysaccharide molecules.

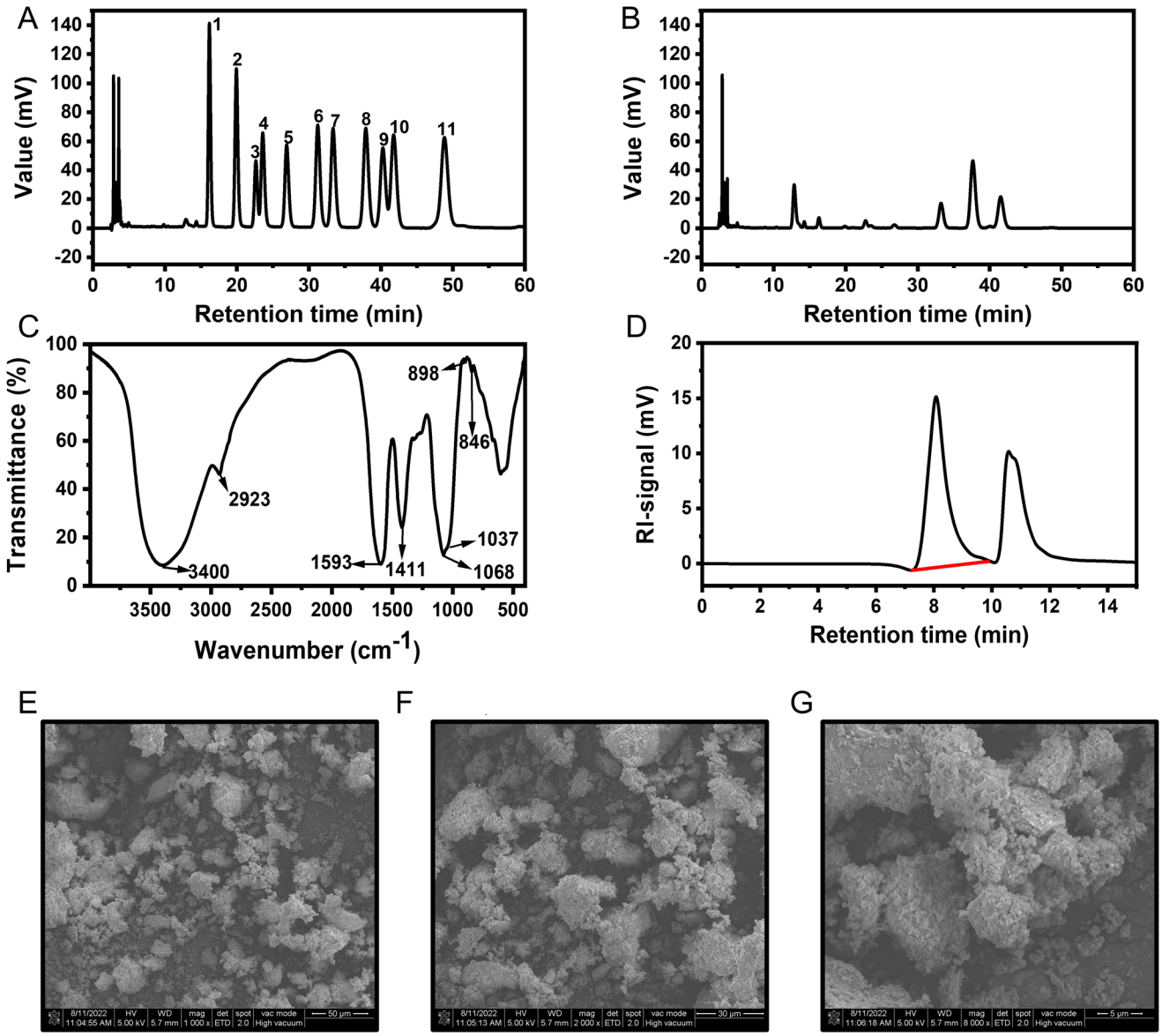


Fig. 1 Chemical characterization of MOLP. (A) Monosaccharide composition analysis by HPLC of the standard monosaccharides: 1-mannose, 2-D-glucosamine, 3-rhamnose, 4-glucuronic acid, 5-galacturonic acid, 6-D-galactosamine HCl, 7-glucose 8-galactose, 9-xylose, 10-arabinose and 10-fucose. (B) The chromatogram of the monosaccharide composition in MOLP. (C) The FT-IR spectrum of MOLP. (D) The HPGPC elution profile of MOLP. (E–G) Scanning electronic micrograph for MOLP at magnifications of ×1000, ×2000 and ×8000.

 

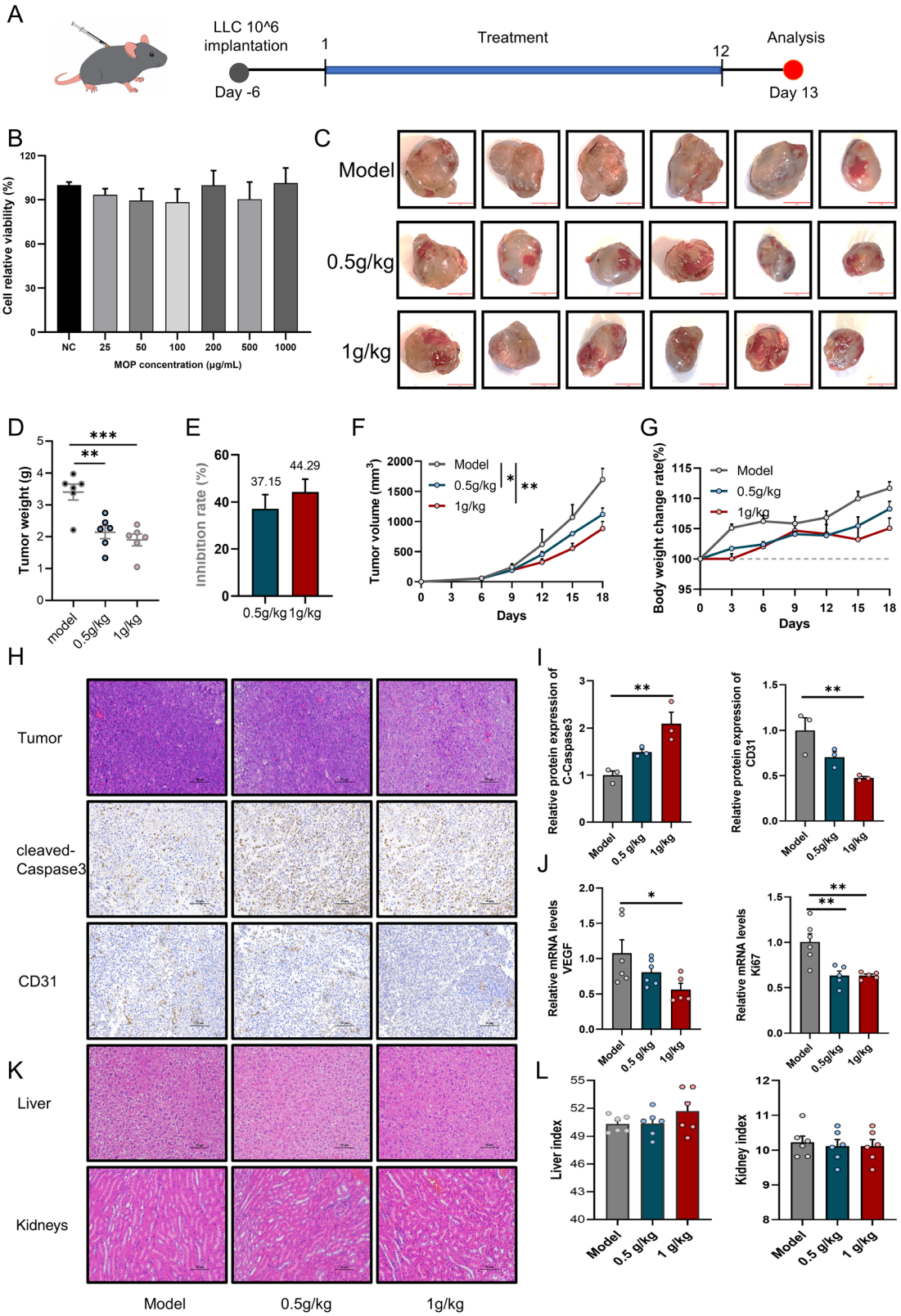


**Fig. 2** The anti-tumor effect of MOLP on LLC-bearing mice ($n$ = 6). (A) Schematic of the experimental design (B) and cell viability of LLC after incubation at different MOLP concentrations. (C) Tumor image. (D) Tumor weight. (E) Tumor suppression rate. (F) Tumor volume. (G) Body weight change rate. (H) Immunohistochemical analysis and H&E staining images of the tumor ($n$ = 3). (I) Immunohistochemical statistics ($n$ = 3). (J) Statistical results of VEGF and Ki67 mRNA levels relative to the model group. (K) H&E staining images of the tumor liver and kidney tissues. (L) The orange index error bars are represented as means ± SEM. *$p$-value <0.05, **$p$-value <0.01, ***$p$-value <0.001. Scale bar, 50 μm.

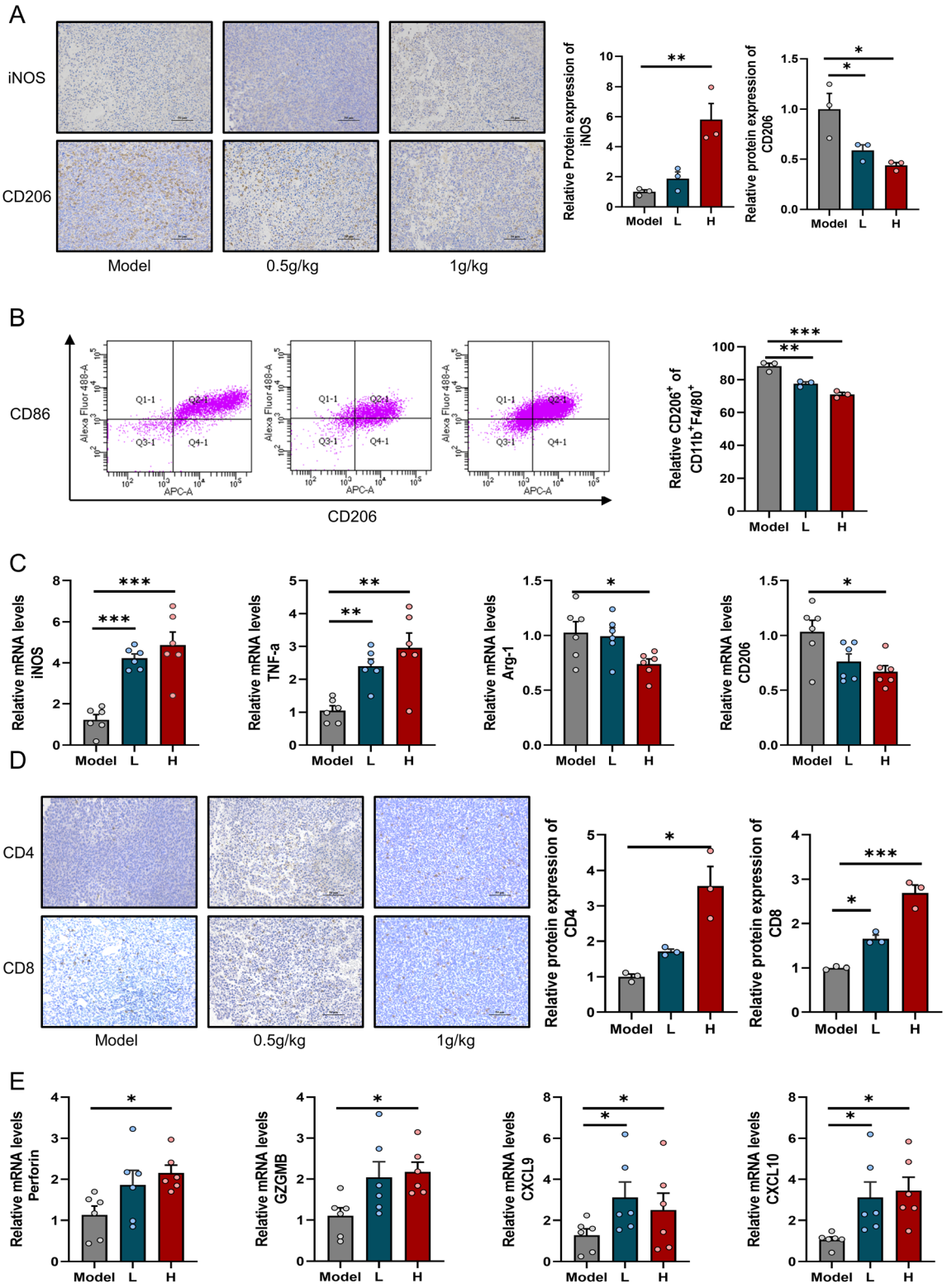


**Fig. 3** Effect of MOLP on the immune cells of LLC tumor-bearing mice. (A) Immunohistochemical images and statistical results of the macrophage polarization markers in the tumor tissues ($n$ = 3). (B) Flow analysis of the macrophage phenotypes and the statistical results ($n$ = 3). (C) The mRNA levels of the macrophage markers in the tumor tissues ($n$ = 6). (D) Immunohistochemical images and statistical analysis of T cells from the tumor tissues ($n$ = 3). (E) The T cell function and mRNA level expression of the recruitment factors ($n$ = 6). Error bars are represented as means ± SEM. *$p$-value <0.05, **$p$-value <0.01, ***$p$ value <0.001.

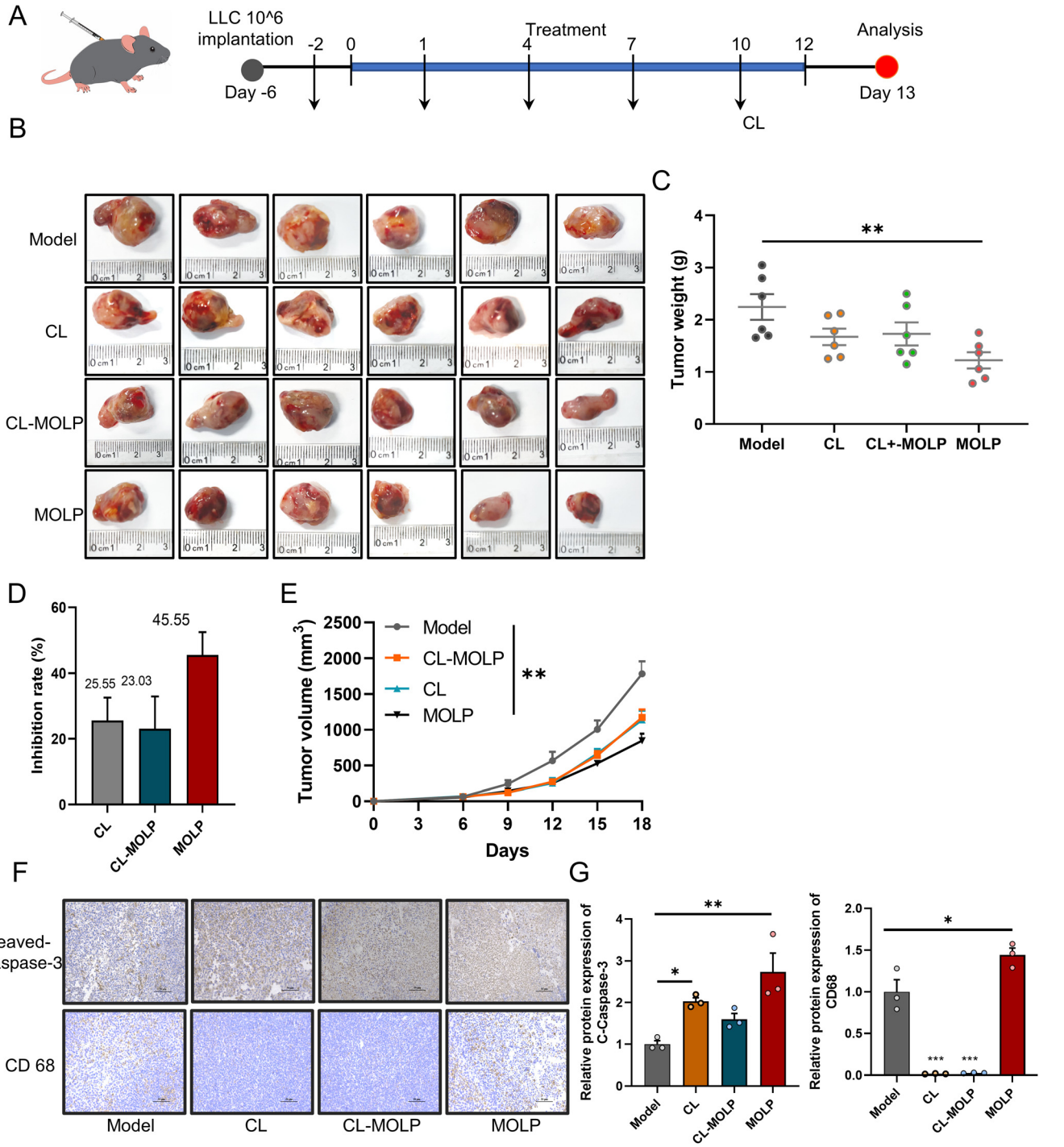


**Fig. 4** MOLP exhibit anti-tumor effects through TAMs ($n$ = 6). (A) Schematic of the experimental design. (B) Tumor image. (C) Tumor weight. (D) Tumor suppression rate. (E) Tumor volume. (F) Immunohistochemical analysis of the tumor tissue ($n$ = 3). (G) Immunohistochemical statistics. Error bars are represented as means ± SEM. *$p$-value <0.05, **$p$-value <0.01 and ***$p$-value <0.001. Scale bar, 50 μm.

### 3.2 MOLP inhibit tumor growth in LLC xenograft mouse models

To evaluate the anti-tumor efficacy of MOLP *in vivo*, an LLC tumor-bearing mouse model was constructed. Firstly, it was found that MOLP had almost no inhibitory effect on the viability of LLC in our *in vitro* study (Fig. 2B). Interestingly, we observed significant tumor inhibition in LLC-bearing mice after treatment with MOLP, with approximately 37.15% inhibition in the low-dose group (0.5 g $kg^{-1}$) and 44.29% inhibition in the high-dose group (1 g $kg^{-1}$) (Fig. 2C–F). The findings suggested that the anti-tumor effects of MOLP may be

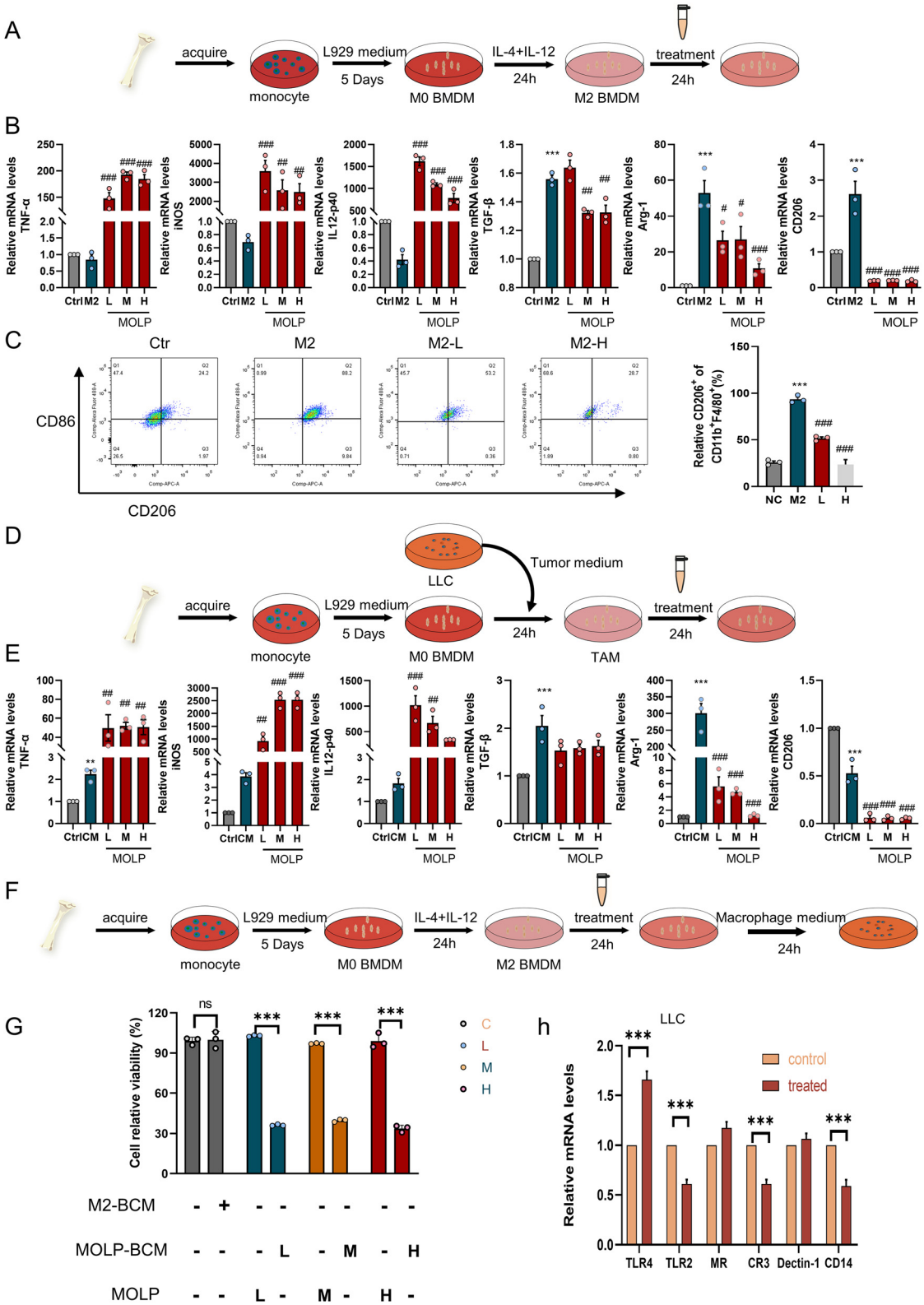


**Fig. 5** *In vitro* study of the effect of MOLP on BMDM polarization ($n$ = 3). (A) Schematic of the experimental design. (B) The effect of MOLP on M1/M2 phenotype genes in IL-4 + IL13-induced M2 BMDMs. (C) Flow cytometry analysis of MOLP alters the M1/M2 phenotype of BMDMs. (D) Schematic of the experimental design. (E) The effect of MOLP on M1/M2 phenotype genes in BMDMs with simulated tumor education. (F) Schematic of the experimental design. (G) The MOLP-induced BMDM supernatant or direct drug treatment of LLC cell viability. (H) The effect of MOLP on the pattern recognition receptor mRNA levels in RAW 264.7 cells. Error bars are represented as means ± SEM. *$p$-value <0.05, **$p$-value <0.01 and ***$p$-value <0.001. $^{\#}p$ value <0.05, $^{\#\#}p$-value <0.01, $^{\#\#\#}p$-value <0.001 according to the model group statistics.

due to immunomodulatory effects rather than cytotoxic effects.

To observe the anti-tumor effect of MOLP, we isolated tumor tissues and performed histopathological analysis and immunohistochemical analysis. H&E staining results found that the tumor cell nuclei were loosely arranged, and the division of the nuclei was obviously reduced and the tumor necrotic areas were significantly increased compared with the model group. Caspases belong to a family of proteolytic enzymes that mediate apoptosis and they play a key role in the process of apoptosis. Among them, caspase-3 is a key executor of apoptosis, and its activation is central to apoptosis and it is mainly found in mammals, and cleaved caspase-3 is the activated form of caspase-3. In this study, MOLP significantly increased the expression of cleaved caspase-3 in the tumor tissues of LLC-bearing mice (Fig. 2H and I), proving that MOLP can induce apoptosis and suppress the growth of lung cancer cells *in vivo*. Tumor vascularization is an important condition for tumor development, infiltration, and metastasis. CD31 is an important indicator used to assess tumor angiogenesis and a key marker of endothelial cell tissue, which can be used to evaluate the degree of malignant proliferation of tumors. The immunohistochemical results of tumor tissues revealed that MOLP could reduce the expression of CD31 in tumor tissues (Fig. 2H and I), effectively inhibiting the vascular growth of tumors and blocking the supply of nutrients and oxygen, thus inhibiting tumor growth. The mRNA levels of Ki67 and VEGF in tumor tissues were measured by qRT-PCR, and it was found that MOLP exerted inhibitory effects on both genes (Fig. 2J). Of these, Ki67 is an important indicator of tumor malignant proliferation and VEGF is a key signaling molecule controlling tumor angiogenesis.

Furthermore, the body mass index (Fig. 2G), organ index (liver and kidneys) (Fig. 2L) and H&E (Fig. 2K) staining showed no significant toxicity or negative effects on mice after MOLP administration. Collectively, these results indicate that MOLP show non-toxicity and can serve as an effective anti-cancer drug, and their anti-cancer effect was mainly to inhibit angiogenesis and promote tumor cell necrosis and apoptosis.

### 3.3 MOLP promote TAM polarization to the M1 phenotype in tumor-bearing mice

TME is a complex environment for the survival of tumor cells, in which immune cells are key players in shaping the tumor-suppressive microenvironment. TAMs, as an essential component of immune cells, are usually divided into two subtypes: M1 type and M2 type. The former exhibits typical anti-tumor functions, while the latter promotes tumor cell growth and migration, as well as pro-angiogenic effects.[28] To investigate whether MOLP can polarize TAMs to the M1 phenotype *in vivo*, firstly, iNOS (M1-type marker) and CD206 (M2-type marker) were immunohistochemically stained in tumor tissues (Fig. 3A), and also the ratio of ($CD206^+$/$CD11b^+F4/80^+$ cells) M2 TAMs was analyzed by flow cytometry (Fig. 3B). The results revealed that treatment with MOLP could promote M1-type expression and suppress M2 expression in LLC xenograft tumors. The expression of pro-inflammatory cytokines TNF-α and iNOS was found to be upregulated by MOLP. The expression of the immunosuppressive markers Arg-1 and CD206 was markedly reduced (Fig. 3C). The above data fully illustrate that MOLP can promote the polarization of M2 TAMs to the M1 phenotype.

To further confirm whether MOLP play an anti-tumor role by regulating the phenotype polarization of TAMs, a macrophage-depleted LLC tumor-bearing mouse model was constructed (Fig. 4A). The results revealed no significant difference between the CL group and the CL-MOLP group (Fig. 4B–E), and the suppressive effect of CL-MOLP on tumor growth was less than that of the MOLP group; this was mainly attributed to the depletion in TAMs. Cleaved caspase-3 is a critical protein for apoptosis. Immunohistochemical staining of the tumor tissues for cleaved caspase-3 revealed that the expression of the protein in the CL-MOLP group was lower than that in the MOLP group (Fig. 3F and G). Immunohistochemical results of the tumor tissues showed that CD68, as the marker of macrophages, was hardly expressed in the CL group and CL-MLOP group, which confirmed the success of model construction (Fig. 3F and G). These outcomes, on one hand, indicated that MOLP can promote macrophage polarization, and on the other hand, indicated that depletion of macrophages in tumor-bearing mice can weaken the tumor suppressive effect of MOLP, suggesting that the anti-tumor effects of MOLP are partly due to the polarization of macrophages.

### 3.4 MOLP promote macrophage polarization to the M1 phenotype *via* TLR4

Given that the above results suggest that the anticancer effect of MOLP was partly based on the polarization of TAMs, we assessed whether MOLP could act directly on macrophages by cellular assays. First, as shown in Fig. 5A and discussed in section 2.4, the mature BMDMs were induced into the M2 phenotype. The marker genes of the M2 phenotype (TGF-β, Arg-1 and CD206) *versus* the M1 phenotype (iNOS, TNF-α and IL12-p40) were assessed at the mRNA level (Fig. 5B). The results revealed a significant decline of M1 phenotype-related genes and a significant increase in M2 phenotype-related genes after induction into M2 BMDMs compared to the untreated M0 BMDMs; successful modeling of M2 BMDMs was additionally verified by flow cytometry (Fig. 5C). Then, by treating M2 BMDMs with MOLP, we found that the expression of M2 BMDM marker genes was remarkably decreased, whereas the expression of M1 marker genes was dramatically increased. The flow cytometry results also revealed that the proportion of M2 BMDMs among macrophages was considerably lower. The above results confirmed that MOLP prompted the induction of M2 macrophages to M1 macrophages.

Given the tumor-promoting effects of M2 TAMs *in vivo*, to simulate the TAMs, the LLC serum-free supernatant was gathered and used as a conditioned medium (CM), as shown in Fig. 5D. The CM-treated BMDMs showed an increase in both M1 and M2 marker genes (Fig. 5E), with extremely increased

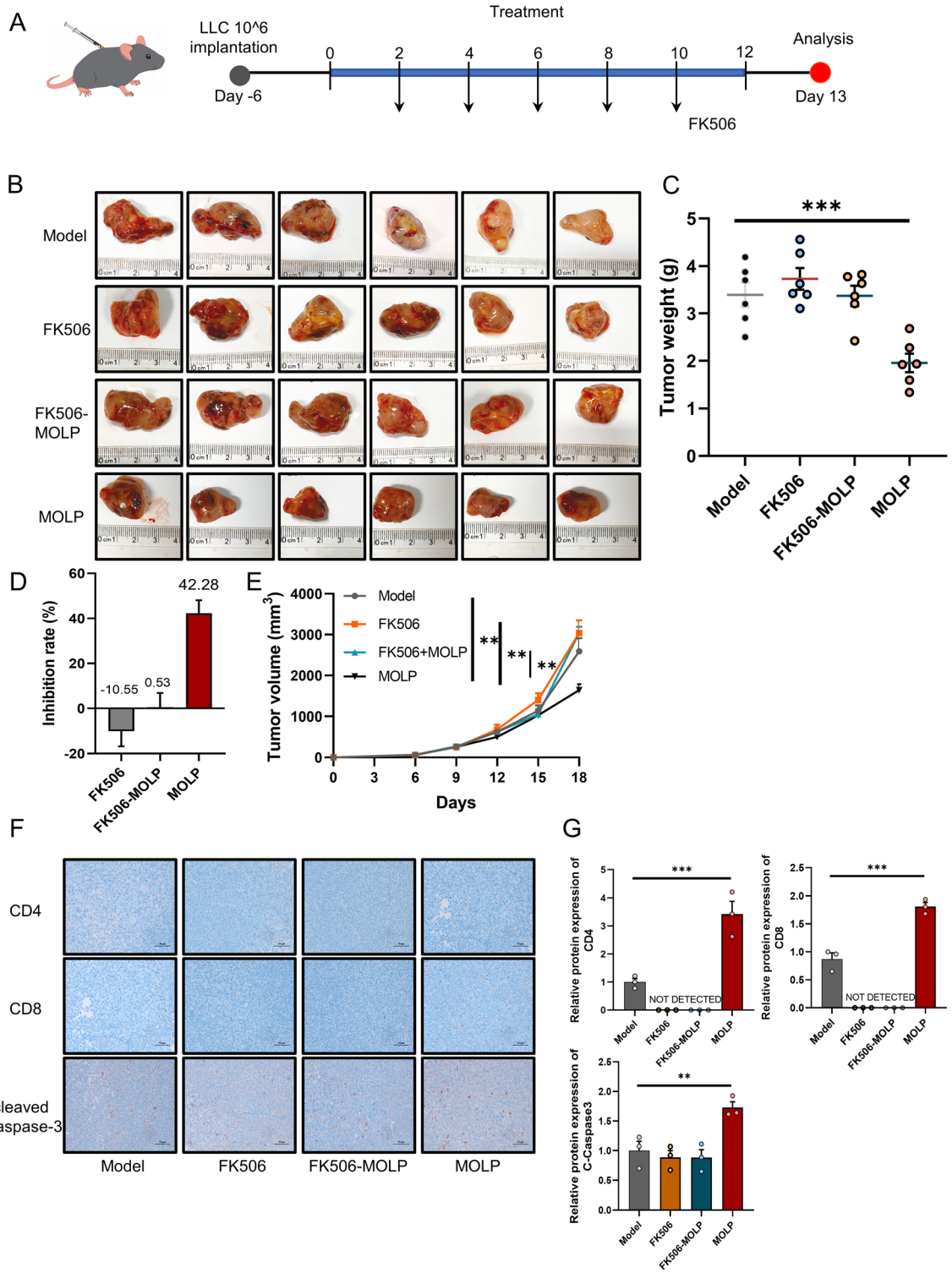


**Fig. 6** MOLP exhibit anti-tumor effects through T cells ($n$ = 6). (A) Schematic of the experimental design. (B) Tumor image. (C) Tumor weight. (D) Tumor suppression rate. (E) Tumor volume. (F) Immunohistochemical analysis of the tumor tissue ($n$ = 3). (G) Immunohistochemical statistics. Error bars are represented as means ± SEM. *$p$-value <0.05, **$p$-value <0.01 and ***$p$-value <0.001. Scale bar, 50 μm.

level of the M2 marker gene *Arg-1*, since the simulated TAMs were macrophages associated with a specific pathological condition, and their activation status resembles that of M2 macrophages. However, TAMs are not only a distinct population of M2 myeloid cells, but also have both M1 and M2 characteristics. Tumor-educated BMDMs treated with MOLP

showed a significant increase of M1 marker genes and achieved reduction of M2 genes. *In vitro* studies demonstrated that MOLP can induce the polarization of M2-like TAMs to the M1 type, which is consistent with the effect of MOLP on RAW 264.7 cells (Fig. S1 and S2†).

For the purpose of investigating whether MOLP can have antitumor effects by driving the conversion of M2 macrophages to M1, we first studied the inhibitory effect of MOLP on LLC cells (Fig. 2B), and found that MOLP had no inhibitory effect on LLC cell viability. Next, we collected the supernatant (BCM) of M2 BMDMs and drug-treated M2 BMDMs to determine the cell viability of LLC cells by the CCK-8 method (Fig. 5F), which indicated that the BCM of M2 BMDMs had no impact on LLC cell viability, whereas the supernatant of M2 BMDMs treated with MOLP explicitly inhibited cell viability (Fig. 5G). The above *in vitro* results indicated that MOLP can convert M2 macrophages to the M1 type and thus play a suppressive role in the viability of LLC cells.

Since polysaccharides are macromolecules that cannot directly penetrate cell membranes, it is impossible for polysaccharides to regulate immune responses and intracellular events through interactions with target molecules within macrophages.[29] Through in-depth studies, polysaccharides were found to intervene in the activation of immune response and play an immunomodulatory role by specifically binding to pattern recognition receptors (PRPs) of macrophages. The PRPs can recognize plant polysaccharides (mainly TLR2, TLR4, Dectin-1, CR3, CD14, and MR).[30] We determined the mRNA levels of the relevant PRPs in RAW 264.7 cells affected by MOLP and found that the TLR4 expression level was significantly increased (Fig. 5H); this is mainly caused by the specific binding of TLR4 to polysaccharides. All the above data suggest that MOLP may shift the macrophage phenotype towards the M1 phenotype by targeting the macrophage TLR4 receptor, and releasing pro-inflammatory factors to suppress tumor activity.

### 3.5 Increased T-cell infiltration and function are essential for the anti-tumor activity of MOLP

T cells, as essential components of immune cells, play indispensable roles in the immunotherapy of tumors. The amount of infiltrating T cells in tumors is closely related to the survival benefits of patients with tumors and the response to immunotherapy.[31] As major immunosuppressive cells in tumor tissues, PD-L1 is overexpressed on TAMs from several cancer tissues. The ligand binds to PD-1, which is expressed on effector T cells, and can inhibit T cell receptor (TCR) signaling, thereby suppressing T cell function and contributing to apoptosis.[32] The previous study proved that MOLP effectively reversed immunosuppressive M2 TAMs to the M1 phenotype. We next studied whether MOLP have an impact on effector T cells, and interestingly, tumor tissues of LLC-bearing mice stained for CD4 and CD8 were analysed by immunohistochemical analysis after MOLP were given orally, and we found that MOLP significantly recruited more $CD4^+$ and $CD8^+$ T cells in the tumor tissue (Fig. 3D). CXCL9 and CXCL10 are important chemokines released by immune cells to recruit T cells. By measuring the expression of *CXCL9* and *CXCL10* genes in tumor tissues, we found that the levels of these chemokines were significantly increased, as seen in Fig. 3E. This also explained that MOLP alleviated the pressure of immunosuppression in the TME. Perforin and granzyme B are critical cytokines for tumor cell killing by CTL, and their corresponding mRNA levels were notably higher than those in the model group (Fig. 3E). Collectively, after treatment with MOLP, LLC-bearing mice improved the immunosuppressive environment, prompted TAMs to release chemokines that recruit T cells, and restored the T cell function to inhibit tumor growth.

FK506 was then used to inhibit T cell activation to investigate whether MOLP exert antitumor effects through T cells. In line with the expected results, the FK506 treatment significantly reduced the tumor suppressive effect of MOLP (Fig. 6B–E). Furthermore, FK5086 significantly reduced the infiltration of $CD4^+$ and $CD8^+$ T cells (Fig. 6F and G); these results collectively indicated that the antitumor activity of MOLP largely depends on T cells.

## 4. Discussion

Tumor cells and their microenvironment are functional wholes; they interact with each other and jointly evolve to foster tumorigenesis. TME mainly consists of tumor cells, their surrounding immune cells, fibroblasts and adjacent stromal tissues.[33] TAMs are the main component of immune cells in the TME and are functionally heterogeneous under stimulatory conditions with two main subpopulations, M1 or M2 phenotypes, respectively. M1 macrophages maintain robust antigen presentation capacity and induce intense Th1 responses. In contrast, M2 TAM can exhibit tumor-propelling and immunosuppressive effects through multiple pathways.[34] For example, TAMs can be involved in promoting tumor cell proliferation by secreting EGF and PDGF; participation in tumor invasion and metastasis by releasing pro-tumor cell metastasis factors such as MMPs (*e.g.*, MMP2 and MMP9); engagement in the immune escape of tumor cells by producing IL10, PGE2, and TGFβ; and participation in the growth of tumor microvessels by expressing vascular (lymphatic vessel) growth factors such as vascular endothelial growth factor (VEGF).[35] However, TAMs are phenotypically more inclined to the M2 phenotype, and thus TAMs are critical for the generation of an immunosuppressive TME. Macrophages rely on TGF-β and IL-10 to convert Th1 cells to Th2 cells to reverse the antitumor effects of $CD8^+$ cytotoxic T cells and $CD4^+$ Th1 cells,[36] which is considered as a tumor immune escape mechanism. Research on how to effectively educate M2 TAMs into the M1 phenotype is a hot topic in immunotherapy. Plant polysaccharides have numerous pharmacological effects, primarily including strengthening or activating the immune response, which in turn provides immunomodulatory, antitumor, and other therapeutic effects, the main mechanism of action being their inherent immunomodulatory effect on immune cells,[37]

especially on macrophages. Thus, the study of plant polysaccharides offers a direction for the discovery of new therapeutic drugs.

Previously, some studies demonstrated that MOLP have immunomodulatory properties, and since tumor growth is greatly mediated by immunomodulation, we built an LLC tumor-bearing mouse model and found that tumor growth was restricted by oral administration of MOLP, although we failed to observe an inhibitory effect of MOLP on LLC cells *in vitro*. Such findings were also reported for other plant polysaccharides – for example, *Lachnum* polysaccharides showed no inhibitory effect on S180 cells, but tumor inhibition has been found in *in vivo* experiments.[13]

In the current study, we revealed that MOLP could restrain tumor growth and suppress tumor angiogenesis. By establishing a macrophage depletion model and a T cell suppression model in LLC-bearing mice, we concluded that MOLP exerted anti-tumor effects mainly because MOLP could polarize TAM to the M1 phenotype as well as increase T cell infiltration with enhanced function. Organ indices of mice and H&E staining of the liver or kidneys ensure the safety of MOLP *in vivo*, so it is a safe and effective anti-cancer drug. Similar to the results *in vivo*, in our cellular experiments, MOLP could polarize the tumor education or IL4 + IL13-induced BMDM phenotype to M1 BMDMs by binding to the TLR4 pattern recognition receptor. MOLP boosted the levels of iNOS, 1L-1β and TNF-α and significantly suppressed the levels of the immunosuppressive *TGF-β* and *Arg-1* genes. The treatment of tumor cells with the polarized supernatant significantly inhibited the growth of tumor cells.

Macrophages are important enforcers of innate immunity, allowing them to recognize the pathogen-associated molecular pattern (PAMP) conserved on the surface of pathogenic microorganisms through PRRs such as TLRs expressed on their surface,[38] and to regulate the expression of various immune response genes through downstream signaling pathways to clear pathogens. Evidence suggests that TLR agonists can arrest tumor growth and progression by activating antigen-presenting cells, including macrophages to exert an innate anti-tumor response.[39] Abundant studies have illustrated that plant polysaccharides can activate the intracellular signaling pathway of macrophages mediated by TLR receptors to promote the release of relevant cytokines and exert their immunomodulatory functions. *Dendrobium* polysaccharides have been proven to inhibit multiple tumor growth processes by targeting the TLR2 receptor of TAMs.[40] Similarly, our experimental study found that MOLP could increase the mRNA level in RAW 264.7 cells, which was mainly attributed to the recognition of MOLP by TLR4.

T lymphocytes are the main type of tumor-infiltrating lymphocyte, and can directly kill tumor cells and optimize immune function. However, they are in a suppressed state in the TME, resulting in a low activity of tumor-infiltrating T lymphocytes, and it is important to improve the TME to achieve normal function and a stable number. TAMs serve as the most infiltrated immunosuppressive cells in tumor tissues; T cells interact with TAMs. The interaction between T cells and TAMs is mediated *via* intercellular communication and liquid phase-mediated mechanisms such as cytokines and chemokines. M2 TAMs were proven to produce Arg-1 and TGF-B for suppressing anti-tumor T cell responses, M1 TAMS by secreting CCL5, CXCL9, CXCL10 and CXCL11 for recruiting Th1, Th17, and cytotoxic T cells,[41] and IFN-c excreted by T cells for acting on antigen presenting cells such as macrophages and increasing their expression of MHC II molecules for resetting the phenotype of M2 TAMs.[42] In the present study, we found that MOLP significantly increased the infiltration of $CD4^+$ and $CD8^+$ T cells, in addition to increasing the expression of granzyme B and perforin. We examined the levels of CXCL9 and CXCL10 in tumor tissues, and found that MOLP promoted the expression of these chemokines *in vivo*. After FK506 inhibited the infiltration of T cells, we found that the efficiency of MOLP inhibition of tumor was almost nil. These data demonstrate that the anticancer effect of MOLP mainly lie in the recruitment of T cells by polarizing TAMs to release chemokines, increasing T-cell infiltration, improving the immunosuppressive microenvironment, and restoring T-cell function.

## 5. Conclusion

In the present study, active polysaccharides, MOLP, were obtained from *Moringa oleifera* leaves and their average molecular mass, monosaccharide composition, and microstructure were chemically characterized. Through *in vivo* and *in vitro* experiments, it was established that MOLP promote the polarization of M2 TAMs to the M1 phenotype through TLR4 receptors, alleviate the immunosuppressive microenvironment, inhibit tumor angiogenesis, suppress the supply of nutrients and oxygen required for tumors, restore T cell infiltration in tumor tissues and enhance their cytotoxic function, thus achieving immunomodulatory and anti-tumor effects.

## Author contributions

Shukai Wang: investigation, writing – original draft, and formal analysis. Qian Hu: conceptualization and methodology. Zihao Chang: investigation and methodology. Yuqi Liu: methodology. Ye Gao: methodology. Xiaowei Luo: methodology. Lipeng Zhou: methodology. Yinxin Chen: methodology. Yitong Cui: methodology. Zhaohui Wang: methodology. Baojin Wang: methodology. Ya Huang: methodology. Yue Liu: methodology. Runping Liu: conceptualization, writing – review and editing, and project administration. Lanzhen Zhang: supervision and funding acquisition.

## Conflicts of interest

The authors declare that they have no known competing financial interests or personal relationships that could have appeared to influence the work reported in this paper.

## Acknowledgements

This study was supported by the Longitudinal Research Development Fund Project of Beijing University of Chinese Medicine (2022-ZXFZJJ-001).

## References

1 H. Li, H. Yu, S. Lan, D. Zhao, Y. Liu and Y. Cheng, Aberrant Alteration of Circulating Lymphocyte Subsets in Small Cell Lung Cancer Patients Treated with Radiotherapy, *Technol. Cancer Res. Treat.*, 2021, **20**, 15330338211039948.

2 D. Qian, H. Liu, X. Wang, J. Ge, S. Luo, E. F. Patz, P. G. Moorman, L. Su, S. Shen, D. C. Christiani and Q. Wei, Potentially functional genetic variants in the complement-related immunity gene-set are associated with non-small cell lung cancer survival, *Int. J. Cancer*, 2019, **144**, 1867–1876.

3 W. H. Ban, C. D. Yeo, S. Han, H. S. Kang, C. K. Park, J. S. Kim, J. W. Kim, S. J. Kim, S. H. Lee and S. K. Kim, Impact of smoking amount on clinicopathological features and survival in non-small cell lung cancer, *BMC Cancer*, 2020, **20**, 848.

4 Y. Ni, X. Zhou, J. Yang, H. Shi, H. Li, X. Zhao and X. Ma, The Role of Tumor-Stroma Interactions in Drug Resistance Within Tumor Microenvironment, *Front. Cell Dev. Biol.*, 2021, **9**, 637675.

5 L. Tian, F. Long, Y. Hao, B. Li, Y. Li, Y. Tang, J. Li, Q. Zhao, J. Chen and M. Liu, A Cancer Associated Fibroblasts-Related Six-Gene Panel for Anti-PD-1 Therapy in Melanoma Driven by Weighted Correlation Network Analysis and Supervised Machine Learning, *Front. Med.*, 2022, **9**, 880326.

6 D.-D. Li, M. Zhang, X. Fan, Y.-Z. Chen, B.-F. Chen, Y. Chang, H.-H. Zhong, H.-Y. Jin and Y.-Z. Huang, Biomimetic albumin-modified gold nanorods for photo-thermo-chemotherapy and macrophage polarization modulationhang, *Acta Pharm. Sin. B*, 2018, **8**, 74–84.

7 S. Mafi, B. Mansoori, S. Taeb, H. Sadeghi, R. Abbasi, W. C. Cho and D. Rostamzadeh, mTOR-Mediated Regulation of Immune Responses in Cancer and Tumor Microenvironment, *Front. Immunol.*, 2022, **12**, 774103.

8 H. Wedekind, K. Walz, M. Buchbender, T. Rieckmann, E. Strasser, F. Grottker, R. Fietkau, B. Frey, U. S. Gaipl and M. Rückert, Head and neck tumor cells treated with hypo-fractionated irradiation die via apoptosis and are better taken up by M1-like macrophages, *Strahlenther. Onkol.*, 2022, **198**, 171–182.

9 H. Guo, W. Zhang, Y. Jiang, H. Wang, G. Chen and M. Guo, Physicochemical, Structural, and Biological Properties of Polysaccharides from Dandelion, *Molecules*, 2019, **24**, E1485.

10 Y. Li, X. Wang, X. Ma, C. Liu, J. Wu and C. Sun, Natural Polysaccharides and Their Derivates: A Promising Natural Adjuvant for Tumor Immunotherapy, *Front. Pharmacol.*, 2021, **12**, 621813.

11 H.-Y. Wang, J.-C. Ge, F.-Y. Zhang, X.-Q. Zha, J. Liu, Q.-M. Li and J.-P. Luo, Dendrobium officinale polysaccharide promotes M1 polarization of TAMs to inhibit tumor growth by targeting TLR2, *Carbohydr. Polym.*, 2022, **292**, 119683.

12 Y. Sun, F. Diao, Y. Niu, X. Li, H. Zhou, Q. Mei and Y. Li, Apple polysaccharide prevents from colitis-associated carcinogenesis through regulating macrophage polarization, *Int. J. Biol. Macromol.*, 2020, **161**, 704–711.

13 S. Zong, J. Li, Z. Ye, X. Zhang, L. Yang, X. Chen and M. Ye, Lachnum polysaccharide suppresses S180 sarcoma by boosting anti-tumor immune responses and skewing tumor-associated macrophages toward M1 phenotype, *Int. J. Biol. Macromol.*, 2020, **144**, 1022–1033.

14 Y. Zheng, F. Zhu, D. Lin, J. Wu, Y. Zhou and B. Mark, Optimization of formulation and processing of Moringa oleifera and spirulina complex tablets, *Saudi J. Biol. Sci.*, 2017, **24**, 122–126.

15 C. Li, Z. Dong, B. Zhang, Q. Huang, G. Liu and X. Fu, Structural characterization and immune enhancement activity of a novel polysaccharide from Moringa oleifera leaves, *Carbohydr. Polym.*, 2020, **234**, 115897.

16 Z. Dong, C. Li, Q. Huang, B. Zhang, X. Fu and R. H. Liu, Characterization of a novel polysaccharide from the leaves of Moringa oleifera and its immunostimulatory activity, *J. Funct. Foods*, 2018, **49**, 391–400.

17 N. Blumenkrantz and G. Asboe-Hansen, New method for quantitative determination of uronic acids, *Anal. Biochem.*, 1973, **54**, 484–489.

18 J. A. Lott, V. A. Stephan and K. A. Pritchard, Evaluation of the Coomassie Brilliant Blue G-250 method for urinary protein, *Clin. Chem.*, 1983, **29**, 1946–1950.

19 M. DuBois, K. A. Gilles, J. K. Hamilton, P. A. Rebers and F. Smith, Colorimetric Method for Determination of Sugars and Related Substances, *Anal. Chem.*, 1956, **28**, 350–356.

20 C. Xiong, P. Li, Q. Luo, J. Yan, J. Zhang, X. Jin and W. Huang, Effect of γ-irradiation on the structure and antioxidant activity of polysaccharide isolated from the fruiting bodies of Morchella sextelata, *Biosci. Rep.*, 2020, **40**, BSR20194522.

21 M. Wu, L. Xu, L. Zhao, C. Xiao, N. Gao, L. Luo, L. Yang, Z. Li, L. Chen and J. Zhao, Structural analysis and anticoagulant activities of the novel sulfated fucan possessing a regular well-defined repeating unit from sea cucumber, *Mar. Drugs*, 2015, **13**, 2063–2084.

22 N. Zhang, B. Yang, K. Mao, Y. Liu, B. Chitrakar, X. Wang and Y. Sang, Comparison of structural characteristics and bioactivity of Tricholoma mongolicum Imai polysaccharides from five extraction methods, *Front. Nutr.*, 2022, **9**, 962584.

23 C. Zhou, S. Yin, Z. Yu, Y. Feng, K. Wei, W. Ma, L. Ge, Z. Yan and R. Zhu, Preliminary Characterization, Antioxidant and Hepatoprotective Activities of Polysaccharides from Taishan Pinus massoniana Pollen, *Molecules*, 2018, **23**, 281.

24 N. Panicker, S. Sarkar, D. S. Harischandra, M. Neal, T.-I. Kam, H. Jin, H. Saminathan, M. Langley, A. Charli, M. Samidurai, D. Rokad, S. Ghaisas, O. Pletnikova,

V. L. Dawson, T. M. Dawson, V. Anantharam, A. G. Kanthasamy and A. Kanthasamy, Fyn kinase regulates misfolded α-synuclein uptake and NLRP3 inflammasome activation in microglia, *J. Exp. Med.*, 2019, **216**, 1411–1430.

25 X. Chang, Y. Zhao, X. Yan, J. Pan, K. Fang and L. Wang, Investigating a pathogenic role for TXNDC5 in rheumatoid arthritis, *Arthritis Res. Ther.*, 2011, **13**, R124.

26 L.-L. Zhu, D. Wu, H.-N. Zhang, Q.-Z. Li, Z. Zhang, Y.-F. Liu, S. Zhou, W.-H. Wang, Z.-P. Li and Y. Yang, Effects of Atmospheric and Room Temperature Plasma (ARTP) Mutagenesis on Physicochemical Characteristics and Immune Activity In Vitro of Hericium erinaceus Polysaccharides, *Molecules*, 2019, **24**, 262.

27 W.-T. Yang, C.-Y. Ke, W.-T. Wu, Y.-H. Tseng and R.-P. Lee, Antimicrobial and anti-inflammatory potential of Angelica dahurica and Rheum officinale extract accelerates wound healing in Staphylococcus aureus-infected wounds, *Sci. Rep.*, 2020, **10**, 5596.

28 M. Khasraw, D. A. Reardon, M. Weller and J. H. Sampson, PD-1 Inhibitors: Do they have a Future in the Treatment of Glioblastoma?, *Clin. Cancer Res.*, 2020, **26**, 5287–5296.

29 C. He, H.-Y. Lin, C.-C. Wang, M. Zhang, Y.-Y. Lin, F.-Y. Huang, Y.-Z. Lin and G.-H. Tan, Exopolysaccharide from Paecilomyces lilacinus modulates macrophage activities through the TLR4/NF-κB/MAPK pathway, *Mol. Med. Rep.*, 2019, **20**, 4943–4952.

30 S. Gurusmatika, K. Nishi, E. Harmayani, Y. Pranoto and T. Sugahara, Immunomodulatory Activity of Octenyl Succinic Anhydride Modified Porang (Amorphophallus oncophyllus) Glucomannan on Mouse Macrophage-Like J774.1 Cells and Mouse Primary Peritoneal Macrophages, *Molecules*, 2017, **22**, 1187.

31 W. J. Turbitt, S. D. Collins, H. Meng and C. J. Rogers, Increased Adiposity Enhances the Accumulation of MDSCs in the Tumor Microenvironment and Adipose Tissue of Pancreatic Tumor-Bearing Mice and in Immune Organs of Tumor-Free Hosts, *Nutrients*, 2019, **11**, E3012.

32 S. Su, A. Lei, X. Wang, H. Lu, S. Wang, Y. Yang, N. Li, Y. Zhang and J. Zhang, Induced CAR-Macrophages as a Novel Therapeutic Cell Type for Cancer Immune Cell Therapies, *Cells*, 2022, **11**, 1652.

33 X. Li, J. Feng, Y. Sun and X. Li, An Exploration of the Tumor Microenvironment Identified a Novel Five-Gene Model for Predicting Outcomes in Bladder Cancer, *Front. Oncol.*, 2021, **11**, 642527.

34 X. Zheng, Y. Huang, K. Li, R. Luo, M. Cai and J. Yun, Immunosuppressive Tumor Microenvironment and Immunotherapy of Epstein-Barr Virus-Associated Malignancies, *Viruses*, 2022, **14**, 1017.

35 Y. Feng, Z. Ye, F. Song, Y. He and J. Liu, The Role of TAMs in Tumor Microenvironment and New Research Progress, *Stem Cells Int.*, 2022, **2022**, 5775696.

36 Y. Guo, H. Tsai, L. Zhang and H. Zhu, Mitochondrial DNA on Tumor-Associated Macrophages Polarization and Immunity, *Cancers*, 2022, **14**, 1452.

37 Y. Yang, X. Yin, D. Zhang, J. Lu and X. Wang, Isolation, Structural Characterization and Macrophage Activation Activity of an Acidic Polysaccharide from Raspberry Pulp, *Molecules*, 2022, **27**, 1674.

38 X. Huang, Y. Feng, G. Xiong, S. Whyte, J. Duan, Y. Yang, K. Wang, S. Yang, Y. Geng, Y. Ou and D. Chen, Caspase-11, a specific sensor for intracellular lipopolysaccharide recognition, mediates the non-canonical inflammatory pathway of pyroptosis, *Cell Biosci.*, 2019, **9**, 31.

39 L. Cui, X. Wang and D. Zhang, TLRs as a Promise Target Along With Immune Checkpoint Against Gastric Cancer, *Front. Cell Dev. Biol.*, 2020, **8**, 611444.

40 S. Tao, Z. Ren, Z. Yang, S. Duan, Z. Wan, J. Huang, C. Liu and G. Wei, Different Molecular Weight Polysaccharides From Dendrobium officinale Kimura & Migo on Human Colorectal Cancer and Transcriptome Analysis of Differentially Expressed Genes, *Front. Pharmacol.*, 2021, **12**, 704486.

41 Z. Duan and Y. Luo, Targeting macrophages in cancer immunotherapy, *Signal Transduction Targeted Ther.*, 2021, **6**, 127.

42 A. Valdivia, J. Ly, L. Gonzalez, P. Hussain, T. Saing, H. Islamoglu, D. Pearce, C. Ochoa and V. Venketaraman, Restoring Cytokine Balance in HIV-Positive Individuals with Low CD4 T Cell Counts, *AIDS Res. Hum. Retroviruses*, 2017, **33**, 905–918.

 